

Structural and optical properties of InN/GaN nanodots grown by metalorganic chemical vapor deposition

Wen-Hao Chang*, Lin Lee, Ching-Yu Chen, Wen-Che Tsai, Hsuan Lin, Wu-Ching Chou, Ming-Chih Lee, and Wei-Kuo Chen**

Department of Electrophysics, National Chiao Tung University, Hsinchu 300, Taiwan

Received 5 October 2007, revised 3 January 2008, accepted 9 January 2008

Published online 2 June 2008

PACS 78.55.Cr, 78.67.Hc, 81.07.Ta, 81.15.Gh

* Corresponding author: e-mail whchang@mail.nctu.edu.tw, Phone: +886-3-5712121ext56111, Fax: +886-3-5715230

** e-mail wkchen@cc.nctu.edu.tw, Phone: +886-3-5712121ext56125

InN nanodots grown on GaN by metalorganic chemical vapor deposition (MOCVD) using conventional growth mode as well as flow-rate modulation epitaxy (FME) at various growth temperatures (550–730 °C) were investigated. We found that different precursor injection schemes together with the effect of growth temperatures greatly influenced the surface morphology of InN dots and their photoluminescence

(PL) properties. The best growth efficiency of InN was achieved by FME at around 650 °C. The residual carrier concentration and PL efficiency was also be improved when a high growth temperature was used. Our results indicated that InN nanodots can be grown at a temperature even higher than 700 °C while maintain their optical quality.

© 2008 WILEY-VCH Verlag GmbH & Co. KGaA, Weinheim

1 Introduction In the past few years, InN thin films with remarkably improved crystalline quality has been realized by techniques of molecular beam epitaxy (MBE) [1] and metalorganic chemical vapor deposition (MOCVD) [2]. It has been shown that the energy gap of InN is around 0.69 eV [3, 4], rather than the previously accepted value of ~1.9 eV. Besides the progress in thin film growth, InN nanostructures, such as nanorods [5] and nanodots [6, 7], have also attracted much attention during the last few years. The nucleation process and structural properties of InN nanodots on various substrates have recently been investigated [8, 9]. However, only a few reports have been addressed on their photoluminescence (PL) properties.

The difficulty in growing high-optical-quality InN arises not only from the large lattice mismatch between InN and substrates, but also from the low decomposition temperature of InN, which is expected to occur at 520–550 °C, leading to a rapid escape of N atoms from the growing surface. If the active nitrogen is insufficient to compensate this decomposition, surface accumulation of metallic In will occur. In MBE growth of InN, this problem may be partially addressed by utilizing low growth temperatures, which is usually below 550 °C. However, the situation for MOCVD growth may be

very different, because the thermal cracking of NH₃ sources is very inefficient at temperatures below 550 °C. In this aspect, a higher growth temperature is essential in MOCVD growth of InN in order to provide more active nitrogen, but the growth temperature is still limited to around 700 °C, due to the desorption of metallic In.

Our previous works have demonstrated that InN nanodots with good optical quality can also be prepared by the flow-rate modulation epitaxy (FME), which is a modified growth technique of MOCVD, wherein the In and N source precursors were supplied alternately [6, 7]. In this study, we focus on the effect of growth temperature on the formation and PL properties of the InN/GaN dots grown by FME and by the conventional MOCVD method (i.e., a continuous growth mode). We found that InN nanodots can be grown at a temperature higher than 700 °C while maintain their optical quality. The interplay among the NH₃ cracking efficiency, surface migration of adatoms, decomposition of InN and In desorption in different precursor injection schemes are discussed.

2 Experimental Samples were grown on sapphire (0001) substrates in a MOCVD system using trimethylgal-

lium (TMGa), trimethylindium (TMIn) and ammonia (NH_3) as source precursors. The growth pressure was held at 200 mbar. After the growth of a 1- μm -thick undoped GaN buffer layer at 1120 °C, the substrate temperature was then lowered to 550–730 °C to grow InN nanodots. Two sets of samples have been prepared using FME and conventional MOCVD methods at different growth temperatures (T_g). In FME, the gas flow sequence in one cycle consists of four steps: a 20-sec TMIn step, a 20-sec NH_3 step, and two 10-sec purge steps of N_2 carrier gas intervened in between. The TMIn and NH_3 flow rates were 150 and 18,000 sccm, respectively, corresponding to molar flow rates of 15.3 and 8.04×10^5 $\mu\text{mol}/\text{min}$. During the TMIn step, a small amount of NH_3 (1,000 sccm) was intentionally supplied to suppress the re-evaporation of In atom during this step. The FME growth of InN dots were completed by a total of six cycles for all samples. For the cases of conventional MOCVD growth, continuous flows of 150-sccm TMIn and 10,000-sccm NH_3 were supplied for 120 s. Noted that the total amount of TMIn was the same in both growth methods.

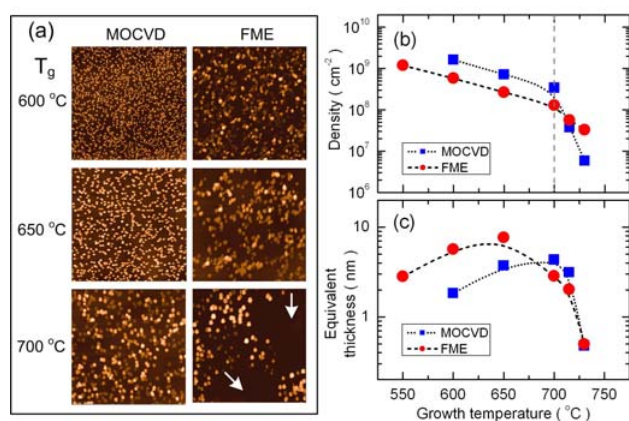


Figure 1 (a) AFM images of InN dots grown at different T_g by FME and by conventional MOCVD. The scanned area for each is $10 \times 10 \mu\text{m}^2$. (b) The corresponding dot density as a function of T_g . (c) The deduced equivalent thickness of the deposited InN.

3 Results and discussion Surface morphologies of InN dots grown by the conventional MOCVD and the FME methods at different T_g are shown in Fig. 1(a). It is clear that the dot size and density are markedly influenced by the growth temperature. In general, the dot size increases whereas the dot density decreases with the increasing T_g . The variation of dot density as a function of T_g is depicted in Fig. 1(b). For the conventional MOCVD growth, two temperature regions divided at about 700 °C were displayed. In the low temperature region ($T_g \leq 700$ °C), the dot density decreases gradually from 7.5×10^9 to $5.0 \times 10^8 \text{ cm}^{-2}$. In the high temperature region ($T_g > 700$ °C), the dot density decreased rapidly and eventually dropped to zero at $T_g = 750$ °C. For FME growth, the dot density also decreases with the increasing T_g , but displaying a less rapid decreasing trend in the high temperature region.

According to the measured surface morphology, the effective growth rate can be estimated. This can be done by deducing the equivalent thickness of the deposited InN according to the average height, diameter and density of InN dots. Such results are shown in Fig. 1(c). One can see that the highest growth rate was achieved by the FME method at $T_g = 650$ °C, corresponding to a growth rate of ~ 300 nm/hr. The conventional growth generally shows lower growth rate in the low temperature region and exhibits a maximum at $T_g = 700$ °C. However, the growth rate for both growth modes decreases rapidly when $T_g > 700$ °C.

As mentioned earlier, the InN growth is controlled by the following three factors: (i) the decomposition of InN, (ii) the thermal cracking of NH_3 and (iii) the desorption of metallic In from the growing surface. Because all the three factors are temperature dependent, the different behaviors of surface dot morphologies grown by different methods, and their dependence on T_g , can be understood from the interplay among these factors together with the different precursor injection schemes. In the low temperature region, the growth of InN is controlled by the amount of active nitrogen. Therefore, both growth methods show increased growth rate with the increasing T_g , due to the enhanced thermal cracking of NH_3 . For $T_g > 700$ °C, the growth of InN becomes limited by high temperature effects, such as In desorption and parasitic reactions, leading to a rapid decrease in growth rate for both growth methods. It is noteworthy that the growth rate of FME starts to decrease for $T_g > 650$ °C, which is lower than that for the conventional method. In FME, the growth of InN proceeds only in the TMIn step, during which the background NH_3 flow was kept at only 1/10 of that used in continuous growth mode. With the increasing T_g , the small amount of background NH_3 become unable to compensate the thermal decomposition of InN during the TMIn step. As can be seen from the surface morphology shown in Fig. 1(a), FME growth at $T_g > 650$ °C shows some void area (as indicated by arrow), which is very likely to arise from such decomposition of InN and re-evaporation of In. On the contrary, this decomposition of InN is expected to be less significant in the conventional MOCVD growth for $T_g \leq 700$ °C, due to the continuous supply of a high NH_3 flow rate. We also noted that the growth rate of the conventional growth mode is slower than that of the FME method for $T_g < 700$ °C, most likely caused by parasitic gas phase reactions between hydrides and In based metalorganic compounds, which may be severe due to the simultaneous injections of group-III and group-IV precursors.

The PL spectra for the InN dots grown by FME and MOCVD measured at 10 K are displayed in Figs. 2(a) and 2(b), respectively. No PL signal was observed for samples grown at 550 °C. For samples grown at $T_g \geq 600$ °C, near-infrared PL emission bands can be observed in the range of 0.76–0.80 eV. A red shift of the PL peak with the increasing T_g can be seen for both FME- and MOCVD-grown samples. Since the sizes of these InN dots are quite large, (with typically dot height > 20 nm), the energy shift caused

by quantum confinement can be neglected. Therefore, differences in peak energy between samples are mainly due to variations of the background electron concentration in the InN dots.

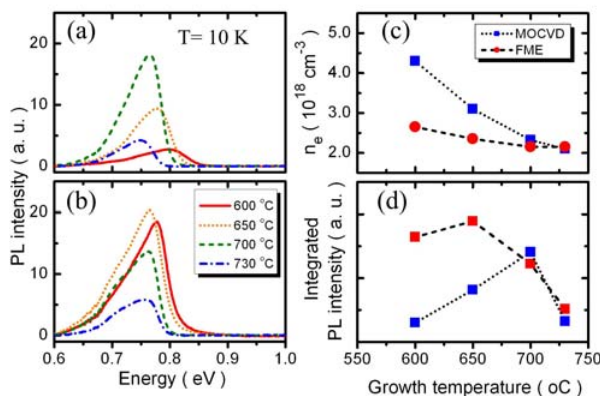


Figure 2 The PL spectra of InN dots grown by (a) MOCVD and (b) FME at various T_g from 600 to 730 °C. (c) and (d) are the deduced carrier concentrations from lineshape model and the integrated PL intensity as functions of T_g , respectively.

To give a quantitative estimation, we have employed a lineshape model considering “free-to-bond” radiative recombination to analyze the PL spectra [10]. Since our main interest aims at finding the Fermi energy and hence the relative electron concentration (n_e) in different samples, the lineshape model was further simplified by assuming a delta-like function for the energy distribution of photogenerated holes near the valance band edge. In this way, the lineshape of the PL emission band can be approximated by the electron energy distribution in the conduction band [7]. This simplified model reproduces our PL spectra very well, and the deduced n_e as a function of T_g is shown in Fig. 2(c). In general, a lower background carrier concentration in InN can be obtained by using a higher T_g , most likely related to a more efficient cracking of NH_3 . We also found that the background carrier concentration of FME grown samples is lower than those grown by conventional method for $T_g < 700$ °C. Since the NH_3 flow rate used in conventional growth mode is significantly higher than that used during the TMIn step of FME, we suspect that some donor-type impurities are incorporated when a high NH_3 flow rate was used.

In Fig. 2(d), the integrated PL intensity as a function of T_g was displayed. A correlation between the PL intensity and the amount of deposited InN shown in Fig. 1(d) can be seen. If we normalize the PL intensity to the amount of deposited InN, the PL efficiency as function of T_g can be obtained, which is shown in Fig. 3. One can see that a better PL efficiency can be achieved at higher T_g for both growth methods. Such an improvement in PL efficiency provides a new approach to the fabrication of high optical quality InN dots for practical applications.

4 Conclusion In summary, the effect of growth temperature on the formation and PL properties of the

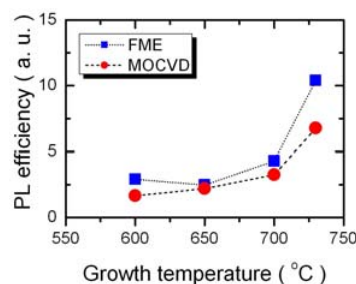


Figure 3 The PL efficiency as function of growth temperature. The PL efficiency is obtained by normalizing the measured PL intensity to the amount of deposited InN.

InN/GaN dots grown by FME and by the conventional MOCVD method have been studied. In FME growth of InN, the highest growth rate can be achieved at $T_g = 650$ °C. We found that InN growth is still attainable at $T_g > 700$ °C while maintain its optical quality, but at the expense of lower growth efficiency. Our results also suggest that a higher growth temperature is beneficial for both reducing the residual carrier concentration and enhancing PL efficiency.

Acknowledgements This work is supported in part by the project of MOE-ATU and the National Science Council of Taiwan under grant No. NSC 96-2112-M-009-006, NSC 95-2112-M-009-044-MY3, NSC 96-2112-M-009-026-MY3, and NSC 96-2112-M-009-014.

References

- [1] H. Lu, W. J. Schaff, J. Hwang, H. Wu, G. Koley, and L. F. Eastman, *Appl. Phys. Lett.* **79**, 1489 (2001).
- [2] A. Yamamoto, T. Tanaka, K. Koide, and A. Hashimoto, *phys. stat. sol. (a)* **194**, 510 (2002).
- [3] V. Yu. Davydov, A. A. Klochikhin, R. P. Seisyan, V. V. Emtsev, S. V. Ivanov, F. Bechstedt, J. Furthmüller, H. Harima, A. V. Mudryi, J. Aderhold, O. Semchinova, and J. Graul, *phys. stat. sol. (b)* **229**, R1 (2002).
- [4] J. Wu, W. Walukiewicz, K. M. Yu, J. W. Ager III, E. E. Haller, H. Lu, W. J. Schaff, Y. Saito, and Y. Nanishi, *Appl. Phys. Lett.* **80**, 3967 (2002).
- [5] C.-H. Shen, H.-Y. Chen, H.-W. Lin, S. Gwo, A. A. Klochikhin and V. Yu. Davydov, *Appl. Phys. Lett.* **88**, 253104 (2006).
- [6] W. C. Ke, C. P. Fu, C. Y. Chen, L. Lee, C. S. Ku, W. C. Chou, W.-H. Chang, M. C. Lee, W. K. Chen, W. J. Lin, and Y. C. Cheng, *Appl. Phys. Lett.* **88**, 191913 (2006).
- [7] W. C. Ke, L. Lee, C. Y. Chen, W. C. Tsai, W.-H. Chang, W. C. Chou, M. C. Lee, W. K. Chen, W. J. Lin, and Y. C. Cheng, *Appl. Phys. Lett.* **89**, 263117 (2006).
- [8] L. Zhou, T. Xu, D. J. Smith, and T. D. Moustakas, *Appl. Phys. Lett.* **88**, 231906 (2006).
- [9] J. G. Lozano, A. M. Sánchez, R. García, D. González, D. Araújo, S. Ruffenach, and O. Briot, *Appl. Phys. Lett.* **87**, 263104 (2005).
- [10] B. Arnaudov, T. Paskova, P. P. Paskov, B. Magnusson, E. Valcheva, B. Monemar, H. Lu, W. J. Schaff, H. Amano, and I. Akasaki, *Phys. Rev. B* **69**, 115216 (2004).